Amino Acids (2010) 39:1363–1367
DOI 10.1007/s00726-010-0590-7

ORIGINAL ARTICLE

In situ fabrication and electrochemical behavior of amino acid polyoxometalate nanoparticles-embedded microcapsules

Dawei Fan · Yongming Deng · Jingcheng Hao

Received: 31 December 2009 / Accepted: 31 March 2010 / Published online: 13 April 2010

Abstract Amino acid polyoxometalate nanoparticles-embedded microcapsules were in situ fabricated by layer-by-layer (LbL) self-assembly method [polyoxometalate, $H_3PMo_{12}O_{40}{\cdot}nH_2O$ (PMo_{12}); amino acid, glycine (Gly)]. The morphology of the obtained microcapsules was characterized by transmission electron microscopy and scanning electron microscopy. The electrochemical behavior of the amino acid polyoxometalate nanoparticles-embedded microcapsules was studied by cyclic voltammetry. The microcapsules show the pH-dependent properties, indicating that the pH of solution plays an important role in the electrochemical behavior of heteropolyanions.

Keywords Glycine · Polyoxometalate · Layer-by-layer · Self-assembly · Microcapsule

Introduction

Polyoxometalates (POMs) have attracted more and more attention for the potential applications in the domain of electrochemistry, medicine (antiviral, antitumor, antibacterial and anti-HIV activity), catalysis and materials science because of their well-defined structures and unique physicochemical properties (Katsoulis 1998; Müller and Henry 2003; Yamase 2005; Yanagie et al. 2006; Coronado and Day 2004). As the basic units of many biological molecules, amino acids are of great importance in biochemistry and life science. The association between POM clusters and proteins show promising applications in electrochemistry and biochemistry (Rhule et al. 1998; Liu et al. 2000; Wang et al. 2006; Kong et al. 2007; Alizadeh et al. 2006).

Layer-by-layer (LbL) assembly technique has been most widely utilized for the fabrication of tailored capsules owing to its simplicity and flexibility, whereby the capsules are prepared by the sequential deposition of polymers or other components that interact through electrostatic, covalent, hydrogen-bonding or hydrophobic interactions onto template cores, followed by removal of the core particles (Decher 1997; Donath et al. 1998; Peyratout and Dähne 2004; Quinn et al. 2007; Yang et al. 2008; Quinn et al. 2008). In this study, we report that amino acid (glycine, ab. Gly) polyoxometalate ($H_3PMo_{12}O_{40}{\cdot}nH_2O$, ab. PMo_{12}) nanoparticles-embedded microcapsules are in situ fabricated by LbL self-assembly method. The electrochemical behavior of microcapsules was investigated by cyclic voltammetric (CV) measurements with changing pH value.

Figure 1 shows the molecular structures of poly(allylamine hydrochloride) (ab. PAH) (a), poly(sodium 4-styrenesulfonate) (ab. PSS) (b), glycine (ab. Gly) (c) and PMo_{12} (d). PMo_{12} has a Keggin structure in which the central *P* atom is surrounded by a tetrahedron whose oxygen vertices are each linked to one of the four Mo_3O_{13} groups. Each Mo_3O_{13} consists of three MoO_6 octahedra linked in a triangular arrangement by sharing edges, and the four Mo_3O_{13} are linked together by sharing corners (Han et al. 2002).

D. Fan · Y. Deng · J. Hao (✉)
Key Laboratory of Colloid and Interface Chemistry,
Shandong University, Ministry of Education,
Jinan 250100, China
e-mail: jhao@sdu.edu.cn

D. Fan · J. Hao
State Key Laboratory of Solid Lubrication,
Lanzhou Institute of Chemical Physics,
Chinese Academy of Sciences, Lanzhou 730000, China

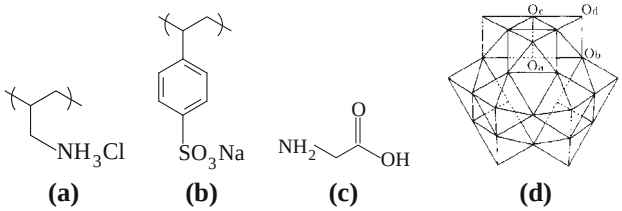

Fig. 1 Molecular structures of PAH (**a**), PSS (**b**), Gly (**c**) and Keggin-type polyanion $[PMo_{12}O_{40}]^{3-}$ (**d** O_a the central oxygen atoms bonded to *P*, O_b corner-shared oxygen atoms, O_c edge-shared oxygen atoms, O_d terminal or skin oxygen atoms)

Materials and methods

Materials

PS-research particles with a diameter of ~450 nm were purchased from microparticles GmbH, Germany. PSS ($M_W = 70{,}000$) and PAH ($M_W = 70{,}000$) were obtained from Sigma–Aldrich Inc., USA. Keggin-type polyoxometalate phosphomolybdic acid ($H_3PMo_{12}O_{40}{\cdot}nH_2O$) was purchased from Alfa Aesar. Glycine was obtained from Amresco, USA. Commercial products were used without further purification. The water used in all experiments was deionized to a resistivity of 18.25 MΩ cm.

Methods

Fabrication of PMo_{12}–Gly nanoparticles-embedded capsules

The negatively charged PS particles as a template were incubated with 3 mL positively charged PAH aqueous solution for 20 min at room temperature, followed by three cycles of centrifugation/rinsing, and finally dispersed in water. The PSS layer was assembled in the same way. The concentration of polyelectrolyte (PAH or PSS) is 2 mg mL^{-1} containing 0.5 mol L^{-1} NaCl. The PAH and PSS adsorption steps were repeated to form $(PAH/PSS)_5PAH$ multilayers on the PS particles to build a smooth and uniform polyelectrolyte layers for self-assembly in situ of PMo_{12}–Gly nanoparticles. Subsequently, alternate adsorption of PMo_{12} and Gly for 30 min with stirring were assembled on $PS/(PAH/PSS)_5PAH$ particles. After adsorption of each layer, the particles were washed three times with deionized water and centrifuged at 9,000 rpm for 5 min. Five cycles of alternate adsorption of PMo_{12} and Gly were carried out to form $PS/(PAH/PSS)_5PAH/(PMo_{12}/Gly)_5$ particles. The concentration of PMo_{12} solution is 0.02 mol L^{-1} containing 0.5 mol L^{-1} NaCl. The pH of the glycine aqueous solution (0.2 mol L^{-1}) was adjusted with dilute hydrochloric acid to 2. Finally, PMo_{12}–Gly nanoparticles-embedded hollow microcapsules were obtained after the template PS core was dissolved in tetrahydrofuran. The LbL assembly process of PMo_{12}–Gly nanoparticles-embedded microcapsules was illustrated in Fig. 2.

Characterization of morphology and CV measurements

Transmission electron microscopy (TEM) observations were carried out at an acceleration voltage of 100 kV (JEM-100 CXIII JEOL). A small amount of sample solution was dropped onto a copper grid (3.02 mm, 250 meshes, coated with Formvar film). After the solution was dried in the air, TEM images were taken on after 10 min.

Scanning electron microscopy (SEM) observations were conducted using a JEOL JSM6700F field-emission scanning electron microscope.

FT-IR (KBr, cm^{-1}) spectra were performed on a Bruker EQUINOX55 FT-IR spectrometer equipped with a DGTS detector for PMo_{12}, glycine and PMo_{12}–Gly nanoparticles-embedded microcapsules.

Cyclic voltammetric (CV) measurements were conducted using a CHI 600B electrochemistry system. A conventional three-electrode system was used, with a bare ITO electrode or a PMo_{12}–Gly nanoparticles-embedded microcapsules coated ITO electrode as a working electrode, platinum foil as a counter electrode, and $Hg/HgCl_2$ as a reference electrode. All of the solutions were deaerated thoroughly with high-purity N_2 for at least 25 min and kept under a pressure of this gas during the experiments.

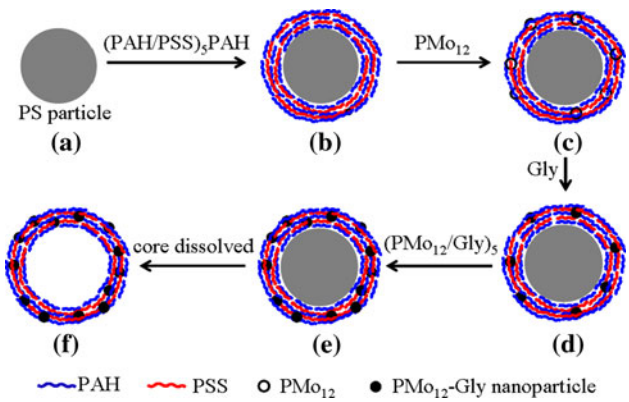

Fig. 2 Illustration of layer-by-layer assembly of PAH, PSS, PMo_{12}–Gly nanoparticles onto PS template particles and hollow microcapsules. The stage shows stepwise deposition of polyelectrolytes on PS colloidal particles (**a**, **b**). In situ assembly PMo_{12}–Gly nanoparticles (**b**–**e**). Decomposition of PS cores and formation of hollow $(PAH/PSS)_5PAH/(PMo_{12}/Gly)_5$ microcapsules (**e** and **f**)

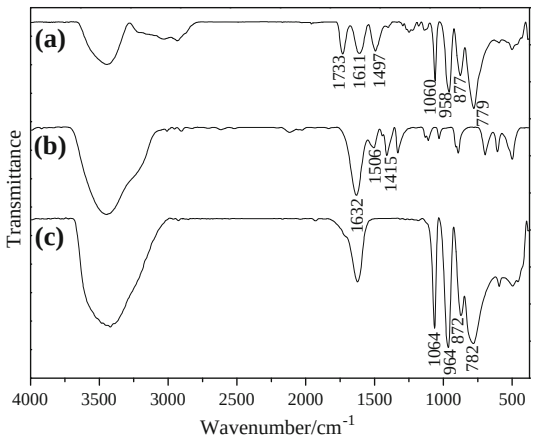

Fig. 3 IR spectra of PMo_{12}–Gly nanoparticles-embedded microcapsules (**a**), glycine (**b**), and PMo_{12} (**c**)

Results and discussion

FT-IR spectra

Figure 3 shows the IR spectra of PMo_{12}–Gly nanoparticles-embedded hollow microcapsules (a), Gly (b) and PMo_{12} (c). In the IR spectra of PMo_{12} (Fig. 3c), the characteristic peaks are vibrational bands of the P–O_a (1,064 cm^{-1}), Mo–O_d (964 cm^{-1}), Mo–O_b(872 cm^{-1}) and Mo–O_c (782 cm^{-1}), respectively. It can be seen from the Fig. 3a, PMo_{12}–Gly nanoparticles-embedded hollow microcapsules showed the similar characteristic peaks to those of the corresponding Keggin-type PMo_{12}, which confirms the PMo_{12} anions in the microcapsules still remain in their Keggin-type structure. The vibrational bands of the P–O_a, Mo–O_d, Mo–O_b and Mo–O_c have red-shifted or blue-shifted, suggesting that interactions between the nitrogen atom of the Gly and the oxygen atoms of the $[PMo_{12}O_{40}]^{3-}$ (Niu et al. 1996; Bi et al. 2001). Amino acid is amphoteric and exits as in the form of the dipolar ion NH_3^+-CH_2-COO^- (namely, inner salt) in crystal. So in the IR spectrum of Gly (Fig. 3b), the characteristic peaks of -COO^- appear at 1,415 cm^{-1}. When Gly reacts with PMo_{12}, the Gly is protonated, and the Gly cation is generated as NH_3^+-CH_2-COOH. Hence, in Fig. 3a, the characteristic peaks of -COO^- disappeared and the characteristic peaks of -COOH (1,733 cm^{-1}) became distinct. The characteristic peaks at 1,611 cm^{-1} should be assigned to vibration of -NH_3^+. We suggest that the $HGly^+$ cations combined with the PMo_{12} anions to form PMo_{12}–Gly nanoparticles-embedded microcapsules.

Morphology measurements of microcapsules

TEM and SEM measurements were conducted for monitoring the morphology and the surface transition of microcapsules. The representative images for bare PS template particles, polyelectrolyte capsules and PMo_{12}–Gly nanoparticles-embedded microcapsules are shown in Fig. 4. The bare PS template particles are smooth ball with diameter of about 450 nm, as shown in Fig. 4a of TEM image and Fig. 4d of SEM image. It can be seen from Fig. 4e of SEM image, the PMo_{12}–Gly nanoparticles-embedded capsules have a lichee-like morphology. In situ assembly of PMo_{12}–Gly nanoparticles on PS/$(PAH/PSS)_5$PAH polyelectrolyte microcapsules results in both an increase in surface roughness and an increase in the diameter of the PS template particles. The mean diameter

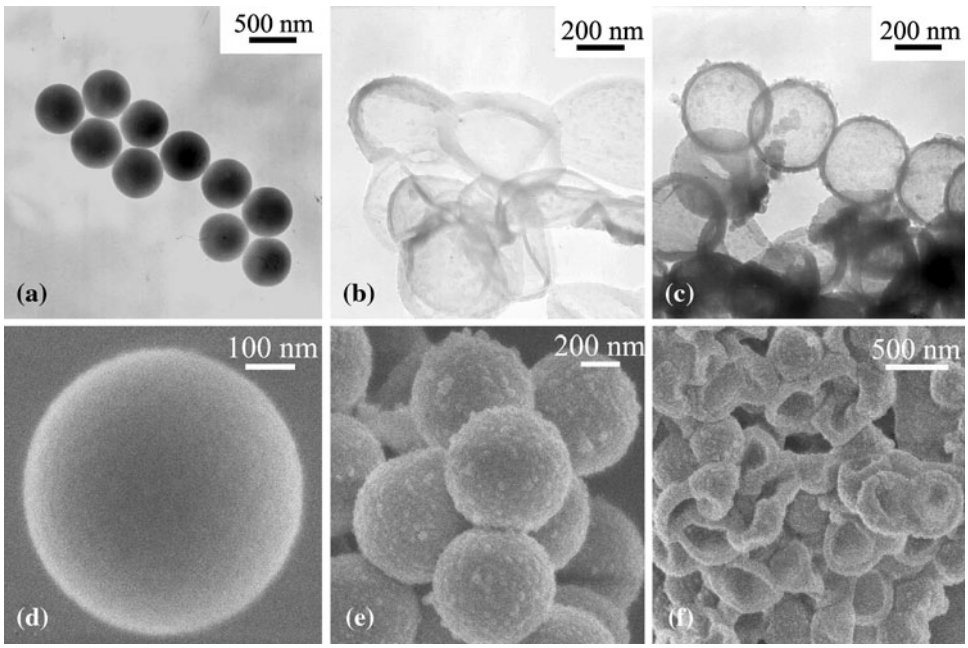

Fig. 4 TEM (**a**–**c**) and SEM (**d**–**f**) images of PS microparticles (**a** and **d**), $(PAH/PSS)_5$PAH polyelectrolyte hollow microcapsules (**b**), $(PAH/PSS)_5PAH/(PMo_{12}/Gly)_5$ microcapsules assembled on PS template (**e**), $(PAH/PSS)_5PAH/(PMo_{12}/Gly)_5$ hollow microcapsules (**c** and **f**)

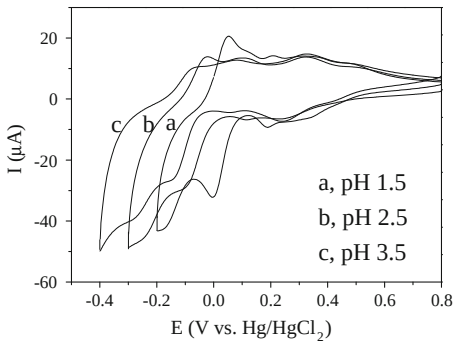

Fig. 5 Cyclic voltammograms of PMo_{12}–Gly nanoparticles-embedded microcapsules modified ITO electrode in 0.5 mol L^{-1} Na_2SO_4–H_2SO_4 buffer solutions with different pH: 1.5 (**a**), 2.5 (**b**), and 3.5 (**c**). Scan rate, 100 mV s^{-1}

of PS/$(PAH/PSS)_5$PAH/$(PMo_{12}/Gly)_5$ particles is 620 nm from SEM image in Fig. 4e, which yields and increase diameter of 170 nm (620 − 450 = 170 nm) than that of the bare PS template particles.

After dissolving the cores by tetrahydrofuran, hollow microcapsules are formed. The TEM image in Fig. 4b displays the dented $(PAH/PSS)_5$PAH hollow polyelectrolyte microcapsules dissolving the core of PS. TEM image of Fig. 4c and SEM image of Fig. 4f show the dented $(PAH/PSS)_5$PAH/$(PMo_{12}/Gly)_5$ hollow microcapsules, respectively. The TEM and SEM images clearly demonstrate that robust and well-defined hollow structures can be obtained after dissolving the bare PS core, no ruptured holes were observed in the hollow microcapsules. The PMo_{12}–Gly nanoparticles-embedded microcapsules could provide potential applications as container or nanoreactor because of the hollow microcapsules keep their original properties of polyoxometalates and amino acids.

Electrochemical behavior

In general, the reduction of the polyoxometalate anions is accompanied by protonation. Hence, the pH of solution plays an important role in the electrochemical behavior of heteropolyanions. Keggin-type polyanion, $[PMo_{12}O_{40}]^{3-}$, are stable in aqueous medium below pH 4 as evidenced by UV–vis spectroscopy. Above this pH value, $[PMo_{12}O_{40}]^{3-}$ anions will be unstable because of hydrolytic decomposition (Li et al. 2002). Figure 5 exhibits the effects of solution pH on the electrochemical behaviors of PMo_{12}–Gly nanoparticles-embedded capsules modified ITO electrode in 0.5 mol L^{-1} Na_2SO_4–H_2SO_4 buffer solutions. It can be seen that the mean peak potentials for all three redox couples are dependent on solution pH and shift in a negative direction with increasing pH values which are within the pH stability range for $[PMo_{12}O_{40}]^{3-}$ anions.

Conclusions

PMo_{12}–Gly nanoparticles were successfully in situ fabricated in the polyelectrolyte capsules. The PMo_{12}–Gly nanoparticles incorporated in capsules were stable enough to maintain their wonderful electrochemical activities of polyoxometalate. The microcapsules show the pH-dependent properties. The amino acid polyoxometalate nanoparticles-embedded microcapsules will show potential applications as container, nanoreactor or drugs delivery in catalysis, biomedicine and so forth.

Acknowledgments This work was financially supported by the NSFC (Grant No. 20625307) and National Basic Research Program of China (973 Program, 2009CB930303).

References

Alizadeh MH, Holman KT, Mirzaei M, Razavi H (2006) Triprolinium 12-phosphomolybdate: synthesis, crystal structure and properties of $[C_5H_{10}NO_2]_3[PMo_{12}O_{40}]\cdot 4.5H_2O$. Polyhedron 25:1567–1570

Bi LH, Wang EB, Huang RD (2001) Synthesis, properties and crystal structure of a novel organic-inorganic salt of 12-silicomolybdate, $(C_2H_5NO_2)_{3.5}H_4SiMo_{12}O_{40}\cdot 8.5H_2O$. J Mol Struct 569:81–88

Coronado E, Day P (2004) Magnetic molecular conductors. Chem Rev 104:5419–5448

Decher G (1997) Fuzzy nanoassemblies: toward layered polymeric multicomposites. Science 277:1232–1237

Donath E, Suknorukov GB, Caruso F, Davis SA, Möhwald H (1998) Novel hollow polymer shells by colloid-templated assembly of polyelectrolytes. Angew Chem Int Ed 37:2201–2205

Han Z, Wang E, Luan G, Li Y, Zhang H, Duan Y, Hu C, Hu N (2002) Synthesis, properties and structural characterization of an intermolecular photosensitive complex: $(HGly\text{-}Gly)_3PMo_{12}O_{40}\cdot 4H_2O$. J Mater Chem 12:1169–1173

Katsoulis DE (1998) A survey of applications of polyoxometalates. Chem Rev 98:359–387

Kong Y, Pan L, Peng J, Xue B, Lu J, Dong B (2007) Preparation and antibacterial activity of nanorod-amino acid polyoxometalates. Mater Lett 61:2393–2397

Li LD, Li WJ, Sun CQ, Li LS (2002) Fabrication of carbon paste electrode containing 1:12 phosphomolybdic anions encapsulated in modified mesoporous molecular sieve MCM-41 and its electrochemistry. Electroanalysis 14:368–375

Liu J, Peng J, Wang E, Bi L, Guo S (2000) A novel amino acid salt of 18-molybdodiphosphate: synthesis and structural characterization of $(Lys)_2H_6[P_2Mo_{18}O_{62}]\cdot 16H_2O$. J Mol Struct 525:71–77

Müller A, Henry M (2003) Nanocapsule water-based chemistry. C R Chim 6:1201–1208

Niu JY, You XZ, Duan CY (1996) A novel optical complex between an organic substrate and a polyoxometalate: crystal and molecular structure of α-$H_4SiW_{12}O_{40}\cdot 4HMPA\cdot 2H_2O$. Inorg Chem 35:4211–4217

Peyratout CS, Dähne L (2004) Tailor-made polyelectrolyte microcapsules: from multilayers to smart containers. Angew Chem Int Ed 43:3762–3783

Quinn JF, Johnston APR, Such GK, Zelikin AN, Caruso F (2007) Next generation, sequentially assembled ultrathin films: beyond electrostatics. Chem Soc Rev 36:707–718

Quinn A, Such GK, Quinn JF, Caruso F (2008) Polyelectrolyte blend multilayers: a versatile route to engineering interfaces and films. Adv Funct Mater 18:17–26

Rhule JT, Hill CL, Judd DA (1998) Polyoxometalates in medicine. Chem Rev 98:327–357

Wang R, Jia D, Zhang L, Liu L, Guo Z, Li B, Wang J (2006) Rapid synthesis of amino acid polyoxometalate nanotubes by one-step solid-state chemical reaction at room temperature. Adv Funct Mater 16:687–692

Yamase T (2005) Anti-tumor, -viral, and -bacterial activities of polyoxometalates for realizing an inorganic drug. J Mater Chem 15:4773–4782

Yanagie H, Ogata A, Mitsui S, Hisa T, Yamase T, Eriguchi M (2006) Anticancer activity of polyoxomolybdate. Biomed Pharmacother 60:349–352

Yang L, Peng H, Huang K, Mague JT, Li H, Lu Y (2008) Hierarchical assembly of organic/inorganic building molecules with π-π interactions. Adv Funct Mater 18:1526–1535